ehp ENVIRONMENTAL HEALTH PERSPECTIVES
http://www.ehponline.org

E2F1-Mediated *FOS* Induction in Arsenic Trioxide–Induced Cellular Transformation: Effects of Global H3K9 Hypoacetylation and Promoter-Specific Hyperacetylation *in Vitro*

Sunniyat Rahman, Zjwan Housein, Aleksandra Dabrowska, Maria Dolores Mayán, Alan R. Boobis, and Nabil Hajji

http://dx.doi.org/10.1289/ehp.1408302

Received: 20 February 2014
Accepted: 6 January 2015
Advance Publication: 9 January 2015

E2F1-Mediated *FOS* Induction in Arsenic Trioxide–Induced Cellular Transformation: Effects of Global H3K9 Hypoacetylation and Promoter-Specific Hyperacetylation *in Vitro*

Sunniyat Rahman,[1] Zjwan Housein,[1] Aleksandra Dabrowska,[1] Maria Dolores Mayán,[2] Alan R. Boobis,[1] and Nabil Hajji[1]

[1]Imperial College London, Centre for Pharmacology and Therapeutics, Department of Medicine, Du Cane Road, London. United Kingdom; [2]Osteoarticular and Aging Research Group, Rheumatology Division, INIBIC-Hospital Universitario, Coruña, Spain

Address correspondence to Nabil Hajji, Imperial College London, Centre for Pharmacology and Therapeutics, Department of Medicine, Du Cane Road, London, W12 0NN, United Kingdom. Telephone: +44 (0) 207 594 7394. E-mail: n.hajji@imperial.ac.uk

Running title: Promoter H3K9ac in As-induced cellular transformation

Acknowledgments: This work was supported by a studentship from the MRC-PHE Centre for Environmental and Health and a MRC Centenary Award received by Mr. Sunniyat Rahman at Imperial College London.

Competing financial interests: The authors do not have any conflict of interest to declare.

Abstract

Background: Aberrant histone acetylation has been observed in carcinogenesis and cellular transformation associated with arsenic exposure, however the molecular mechanisms and cellular outcomes of such changes are poorly understood.

Objective: We investigated the impact of tolerated and toxic As_2O_3 exposure in human embryonic kidney (HEK293T) and urothelial (UROtsa) cells to characterise the alterations in histone acetylation, gene expression and the implications for cellular transformation.

Methods: Tolerated and toxic exposures of As_2O_3 were identified by measurement of cell death, mitochondrial function, cellular proliferation and anchorage-independent growth. Histone extraction, MNase sensitivity assay and immunoblotting were used to assess global histone acetylation levels and gene promoter specific interactions were measured by chromatin immunoprecipitation followed by reverse-transcriptase polymerase chain reaction.

Results: Tolerated and toxic dosages were defined as 0.5 μM and 2.5 μM As_2O_3 in HEK293T cells and 1 μM and 5 μM As_2O_3 in UROtsa cells respectively. Global hypo-acetylation of H3K9 at 72 hours was observed in UROtsa cells following tolerated and toxic exposure. In both cell lines, tolerated exposure alone led to H3K9 hyper-acetylation and E2F1 binding at the *FOS* promoter, which remained elevated after 72 hours contrary to global H3K9 hypo-acetylation. Thus, promoter specific H3K9 acetylation is a better predictor of cellular transformation than global histone acetylation patterns. Tolerated exposure resulted in an increased expression of proto-oncogenes *FOS* and *JUN* in both cell lines at 72 hours.

Conclusion: Global H3K9 hypo-acetylation and promoter-specific hyper-acetylation facilitate E2F1-mediated *FOS* induction in As_2O_3-induced cellular transformation.

Introduction

Arsenic is regarded as one of the most toxic naturally occurring carcinogenic metalloids (Chen et al. 1985; Hajji et al. 2010). Arsenic containing substances can be broadly classified into two groups, organic and inorganic arsenicals, with the latter being considered to be more toxic to human health. Inorganic species such as arsenite [As (III)] and arsenate [As (V)] are primarily ingested through contaminated drinking water leading to negative health outcomes (Grund et al. 2008; 2005). The acute arsenic poisoning dosage ranges from 0.17 - 0.87 mg/kg bw leading to diarrhoea and vomiting in addition to kidney and liver toxicity. Long term exposure to arsenic leads to severe detrimental health outcomes including cardiovascular disease and malignancies of the skin, lung and bladder (Kapaj et al. 2006; Nelson et al. 2006). Although epidemiological studies have extensively characterised the association between chronic arsenic exposure and the rising incidence of malignant based mortality, a mechanistic understanding of arsenic-induced carcinogenicity remains to be established (Kurttio et al. 1999). Proposed mechanisms include the generation of reactive oxygen species, cytotoxicity due to the formation of a reactive metabolite, inhibition of DNA repair, chromosomal aberrations, uncontrolled cellular proliferation and altered DNA methylation patterns (Shi et al. 2004).

A mounting body of evidence suggests that epigenetic mechanisms may play a role in the carcinogenicity of arsenic, not only through aberrant DNA methylation, but through altered expression of microRNAs and changes in histone modifications (Ren et al. 2011). Alterations in DNA methylation in response to arsenic exposure is relatively well documented, from the identification of arsenic as a repressor of DNA methyltransferase expression, to the detection of a number of hypo- and hyper-methylated tumour suppressor and oncogenic promoter loci such as *p15*, *p16*, *p53*, *Hras1*, *Myc* and *Esr1* (Chanda 2006; Reichard and Puga 2010). Increased global

DNA methylation of peripheral blood mononuclear cells has also been observed and correlated with water, urinary and blood arsenic levels in Bangladeshi adults (Niedzwiecki et al. 2013). Beyond DNA methylation little is known about the effects arsenic has on the higher order chromatin structure. An increasing body of evidence suggests that post-translational histone modifications, particularly histone acetylation can influence not only overall chromatin structure but also gene transcription with clear functional consequences in cellular processes such as proliferation and apoptosis (Füllgrabe et al. 2010). Suitably, histone modification alterations as a result of arsenic exposure have been identified particularly changes in phosphorylation, methylation and acetylation but relating such modifications to a mechanistic outcome has been limited (Jo et al. 2009; Li et al. 2002; Zhou et al. 2008).

Arsenic exposure has been shown to increase global histone acetylation via the inhibition of histone deacetylases (HDACs) at an intensity comparable to the HDAC inhibitor triochostatin A (Iacobuzio-Donahue 2009). Two functionally antagonistic enzyme groups mediate histone acetylation, comprising three major families of histone acetyltransferases (HATs) and four classes of histone deacetylases (HDACs). Due to the opposing functional nature of the HDACs and HATs, it has been suggested that the relative balance either through expression or activity, alters the physiology of cells and provides an insight into the pathological outcomes in a number of diseases including cancer (Peserico and Simone 2011). This equilibrium has yet to be studied further in the context of arsenic exposure.

Whilst multiple arsenic species have been used in carcinogenesis studies, the use of low-dose arsenic trioxide (As_2O_3) exposure has proven to be suitable in studies pertinent to cellular transformation and epigenetic aberrations. Low dose (0.01-1 μM) As_2O_3 exposure for 24 hours has been shown to increase proliferation and cell cycle progression in normal breast epithelial

cells (MCF10A) via the elevated expression of CDC6 and cyclin D1 (Liu et al. 2010). Exposure to tolerated As_2O_3 in BALB/c 3T3 cells not only led to cellular transformation and tumour generation in nude mice, but also a time-dependent increase in H3K27 trimethylation mediated by polycomb proteins BM1 and SUZ12 (Kim et al. 2012). Lung epithelial BEAS-2B cells exposed to a tolerated As_2O_3 dosage, also led to an increase in cellular proliferation and the differential expression of genes regulating histone H1, H3 and H4 as determined by an *in silico* pathway analysis (Stueckle et al. 2012). Additional research is required to investigate the carcinogenic mechanisms of As_2O_3, as human exposure to this species of arsenic is not limited to tolerated environmental exposures, but also through cytotoxic anti-cancer therapies (Soignet et al. 1998). Thus comparisons between tolerated and toxic exposures of As_2O_3 require further interrogation.

This study characterised the tolerated and toxic profile of As_2O_3 exposure by analysing multiple cellular survival parameters. For this study, a tolerated exposure was one that induced significant biological effects without causing toxicity, whilst a toxic exposure induced significant biological effects leading to toxicity and cell death. Identification of a tolerated concentration ensured epigenetic characterisation of the relevant cellular context that is of continued proliferation and cellular tolerance rather than toxicity. We also characterised the higher order chromatin conformation and histone acetylation changes that occur from As_2O_3 exposure at tolerated and toxic dosages and between an early to a more prolonged exposure. We explored the impact of As_2O_3 exposure on HDAC and HAT expression and determined if specific alterations in histone acetylation impinge on known proto-oncogenic promoters, altering gene-expression leading to increased proliferation and carcinogenic potential.

Materials and Methods

Cell culture

Human embryonic kidney (HEK) 293T cells and Human urothelial (UROtsa) cells were generously donated by Dr. Bertrand Joseph (Karolinska Institutet) and Prof. Scott Garrett (University of North Dakota) respectively. Cells were grown in T_{75} flasks with Dulbecco's Modified Eagle's Medium (Sigma) completed with 10% fetal bovine serum (Sigma), 1% L-Glutamine (Gibco) and 1% Penicillin-Streptomycin solution (Sigma). All cells were cultured at 37^{o}C in a humid 5% CO_2 atmosphere.

Quantitative real-time PCR

Total RNA was extracted by using the RNeasy Mini Kit (Qiagen) as per the manufacturer's protocol. Two-step quantitative real-time PCR was performed, first by synthesis of cDNA by using the ThermoScript RT-PCR System (Invitrogen) with a 5 μg input RNA amount for each sample. Secondly quantitative real-time PCR was carried out on an ABI7500 Fast Real Time PCR System (Applied Biosystems) with a Platinum SYBR Green qPCR SuperMix-UDG (Invitrogen) used as per the manufacturer's protocol. For quantification, the standard curve method was used which is described in detail by (Bookout et al. 2006). See Supplemental Material, Table S1 for the primers used.

Clonogenic assay

HEK293T cells were seeded into six-well dishes at 500 cells per well and incubated overnight in culture medium. The next day the medium was changed and the arsenic trioxide treatment was started, with no further changes of medium or replenishment. After the exposure period, cells

were washed with PBS and fixed with 100% methanol for 10 minutes at -20^{o}C. Colonies were stained with a 5% Giemsa, 25% methanol and 70% PBS solution and then counted. Clonogenic assay was performed as described previously by us (Hajji et al. 2010).

Proliferation assay

Cells were seeded into a 96-well plate at 4 x 10^3 cells per well and incubated overnight in 100 μL culture medium. After toxicant exposure, 10 μL of Cell Proliferation Reagent WST-1 (Roche) was added to each well and incubated for 4 hours at 37^{o}C and 5% CO_2. Medium was homogenised on a plate shaker for 1 minute before absorbance measurement at 440 nm in a plate spectrophotometer (FLUOstar OPTIMA, BMG Labtech). Absorbance readings were subtracted from a background measurement at 440 nm, which is the absorbance of culture medium with WST-1 in the absence of cells. Data was presented as a proliferative index in arbitrary units.

Anchorage-independent growth

Soft agar plates were prepared using two agar densities. 0.8% Noble Agar (Sigma) was used as the base layer dissolved in H_2O and supplemented DMEM (Sigma) as per cell culture parameters at a 1:1 ratio. Cells were pre-treated with As_2O_3 for the desired duration, plated at a 2.5 x 10^3 density in a 0.4% Noble Agar top layer and fed every 3 days. After 14 days plates were stained with 0.005% Crystal Violet (Sigma) and 20% methanol (Sigma) diluted in 1X PBS (Gibco) for 2 hours. Colonies were examined under a stereomicroscope. Further details regarding this method are described by (Rapits and Vultur, 2001).

Histone extraction

Cells were disrupted on ice in a lysis buffer (10 mM Tris pH = 6.5, 50 mM sodium bisulphate, 10 mM $MgCl_2$, Sucrose 8.6% and 1% Triton X-100)**.** The sample was centrifuged at 10,000 x g for 10 minutes at 4^{o}C. The pellet was washed in ice-cold Tris-EDTA (Tris-EDTA solution: 10 mM Tris pH = 7.4, 13 mM EDTA) and centrifuged. Histones were precipitated by acid-extraction as previously described by us (Hajji et al. 2010).

Western blots

Acetylation of core histones and relative levels of intracellular cellular survival components were detected by immunoblotting. Cell lysates were separated by SDS-PAGE under reducing conditions and transferred to a nitrocellulose membrane (GE Life Science). Membranes were visualised using ECL reagents and exposure to ECL hyperfilm (GE Healthcare). Blots were quantified by densitometry analysis using the ImageJ software (National Institutes of Health, http://rsb.info.nih.gov/ij/) with normalisation against ß-actin and total histone proteins to correct for loading. See Supplemental Material, "Antibodies."

Protein extraction

Total protein extraction was achieved by disrupting harvested cells with TGN buffer (1 M Tris-HCL, 2.5 M NaCl, Glyserol, 0.5 M β-glycerphosphate, Tween 20 and Nonidet P40; completed with EDTA-free protease inhibitor (Roche)). Samples were centrifuged at maximal speed for 10 minutes yielding the proteins in the supernatant.

Flow cytometry

Mitochondrial superoxide anion reactive oxygen species (ROS) was identified in live cells using the MitoSOX Red flourogenic dye according to the manufacturer's guidelines (Invitrogen). Cells were harvested and washed with PBS and suspended into 250 μL of 2.5 mM Mitosox Red (Invitrogen) flourogenic dye dissolved in PBS and allowed to incubate for 20 minutes under cell culture conditions in the dark. Mitochondrial superoxide was measured by flow cytometer (FACSCalibur, BD Biosciences). MitoSOX Red was excited by laser at 488 nm and detected in the FL2 channel.

Mitochondrial membrane potential and apoptosis was assayed by incubating cells after washing in 80 μM $DiOC_6$ and propidium iodide for 20 minutes at 37^{o}C in the dark. The samples were then analysed by a flow cytometer (FACSCalibur, BD Biosciences). Cell cycle analysis of fixed cells was achieved by incubation with 50 μM propidium iodide (Sigma). Cells were fixed by the addition of 70% ethanol. Fluorescence was measured using the FL2 channel on a flow cytometer (FACSCalibur, BD Biosciences). All the data was analysed using Cyflogic Version 1.2.1 (Perttu Terho, Mika Korkeamäki, CyFlo Ltd).

Poly (ADP-Ribose) polymerase 1 (PARP) cleavage

PARP cleavage is a hallmark of apoptosis (Duriez and Shah 1997). It was used as an endpoint to identify toxicity induced by As_2O_3 exposures by western blotting as described previously.

Transfections

Transient transfections were achieved using filter-sterilised polyethylenimine (PEI) reagent (Polysciences) at 1 mg/mL in H_2O, pH 6.8. Transfection reagent and plasmid complex was

synthesised using a 1:4 DNA to PEI weight/volume ratio made up to 200 μL in nude Dulbecco's Modified Eagle's Medium (DMEM) (Sigma) before drop-wise addition to the cells. After transfection cells were rested the next day in fresh DMEM for 24-hours before As_2O_3 exposure. See Supplemental Material, "Plasmids."

Micrococal nuclease (MNase) sensitivity assay

Cells were lysed in NP-40 lysis buffer. Nuclei were resuspended in MNase digestion buffer. A total of 0.025 units of MNase (Sigma – N3755) was added to each sample and incubated at 15-20^{o}C for 5 minutes. The reaction was stopped by the addition of MNase digestion buffer, MNase stop buffer, proteinase K and 20% SDS followed by overnight incubation. DNA was extracted by standard phenol/chloroform extraction and ethanol precipitation. Detailed methods and reagents have been previously described by (Cold Spring Harbor Laboratory Press. 2005).

Chromatin immunoprecipitation

HEK293T and UROtsa cells were exposed to As_2O_3 for 3 and 72 hours and fixed with formaldehyde and quenched with glycine. Chromatin immunoprecipitation of samples were carried out as described previously (Nelson et al. 2006) followed by qRT-PCR. Enrichment of E2F1 in acetylated H3K9 promoters of *TP53, BAX, PUMA, MYC* and *FOS* fragments precipitation was detected with an anti-acetylated H3K9 and anti-E2F1 antibodies respectively. 10% of the sample was set aside as input. C_t values were normalised as per the following equation: ΔC_t[normalised ChIP] = (C_t[ChIP] – (C_t[input] – $\log_2$ (0.1))). The % input was calculated with the following equation: % input = $2^{(-\Delta Ct[\text{normalised ChIP}])}$. See Supplemental Material, Table S2.

Results

Identification of a tolerated and toxic exposure of arsenic trioxide

Two cells lines were used in this study. HEK293T was used as they form a minimal number of colonies under anchorage independent condition, have good tolerance to transfection and a good toxicity response to As_2O_3. UROtsa cells were used as these cells exhibit normal characteristics with no colony formation in soft-agar and are ideal to study environmental insult to the human urothelium and bladder carcinogenesis (Rossi et al. 2001). To ensure characterisation of the appropriate epigenetic context the apoptotic endpoint of PARP cleavage was used to identify tolerated and toxic exposures of As_2O_3 in both HEK293T and UROtsa cell lines. PARP cleavage was observed from 10 μM – 80 μM As_2O_3 for cells treated for 24 hours, and for 2.5 μM As_2O_3 for cells treated for 1-week for HEK293T cells (Figure. 1, A, B). Exposures from 2.5 – 10 μM As_2O_3 demonstrated cytotoxicity after 1-week as assessed by caspase-3 cleavage, truncation of the pro-apoptotic factor BID, p53 stabilisation and activation by phosphorylation at serine 15 (Figure 1, B). No PARP cleavage was observed after a 1-week exposure to 0.5 μM As_2O_3 suggesting that this exposure was tolerated (Figure. 1, C). UROtsa cells treated for 72 hours showed no PARP cleavage when exposed to 1 μM As_2O_3, whilst higher exposures of 5 μM – 10 μM As_2O_3 led to clear PARP cleavage (Figure. 1, D). This allowed us to define a tolerated exposure as 1 μM As_2O_3 and a toxic exposure as 5 μM As_2O_3 for the UROtsa cell line.

HEK293T treated for 72 hours with 0.5 μM As_2O_3 showed no discernable difference compared to the untreated control group in the generation of mitochondrial reactive oxygen species (ROS) or mitochondrial membrane depolarisation ($\Delta\psi_M$) (Figure. 1, E, F). Cell death was similar to control levels as quantified by propidium iodide staining after a 0.5 μM As_2O_3 exposure (Figure.

1, G). In contrast, the 2.5 μM As_2O_3 exposure resulted in a significant increase in mitochondrial ROS, loss of mitochondrial membrane potential and cell death. These analyses allowed us to define a tolerated exposure as 0.5 μM As_2O_3 and a toxic exposure as 2.5 μM As_2O_3 for exposures ≥ 72 hours for the HEK293T cell line.

Cellular proliferation, survival, and anchorage-independent growth in response to a tolerated As_2O_3 exposure

HEK293T cells exposed for 1-week to 0.5 μM As_2O_3 exhibited a significantly increased elevation in cellular proliferation (Figure. 1, H). A significant proliferative elevation was also observed in UROtsa cells exposed to 1 μM As_2O_3 for 72 hours and 1-week (Figure. 1, I). Cell cycle disruption was observed in both cell lines after a 72-hour tolerated As_2O_3 exposure, with an increased percentage of cells passing the G1/S and G2/M checkpoints (Figure. 1, J, K). Analysis by clonogenic assay in HEK293T cells identified positive proliferation and cellular survival after a 0.5 μM As_2O_3 exposure for 15 days (Figure. 1, L, M). A lower dose exposure of 0.25 μM As_2O_3, although tolerated was unable to stimulate positive proliferation. Larger and a significantly increased number of three-dimensional spheroid colonies grew in soft-agar compared to the untreated control after a 12-week 0.5 μM As_2O_3 exposure (Figure. 1, N, O).

H3K9 and H4K12 acetylation and *HDAC2* and *PCAF* mRNA expression profiles in response to As_2O_3.

Two time points were used to identify specific arsenic-induced histone acetylation changes and to evaluate the plasticity of such events with both HEK293T and UROtsa cell lines. At 3 hours, an indicative elevation of H3K9 and H4K12 acetylation upon exposure to 0.5 μM and 2.5 μM As_2O_3 was observed in HEK293T cells (Figure. 2, A). There was no change in H4K16

acetylation. In UROtsa cells a small increase but not significant in H3K9 and H4K16 acetylation was measured after a 3-hour exposure to 1 μM and 5 μM As_2O_3 (Figure. 2, B). Significant H3K9 hypo-acetylation was observed in UROtsa cells after a 72-hour exposure to both tolerated (1 μM) and toxic (5 μM) exposure. A similar but not significant trend was observed in HEK293T cells where both 0.5 μM and 2.5 μM As_2O_3 led to hypo-acetylation of H3K9 after 72 hours.

Transient transfection followed by immunoblotting identified HDAC2 and PCAF as the key enzymes involved in controlling H3K9 acetylation status (Figure. 2, C, D). Transfection with PCAF elevated H3K9 acetylation relative to the control, and treatment with 0.5 μM As_2O_3 for 3-hours synergised this effect with enhanced acetylation of H3K9 (Figure. 2, D).

Using quantitative real-time PCR, dosage-specific expression effects were measured for HDAC2. After 3 hours where both dosages are tolerated, HDAC2 expression is significantly suppressed only at the 2.5 μM As_2O_3 dosage (Figure. 2, E). In contrast after 72 hours of exposure HDAC2 expression level is significantly elevated only at the tolerated 0.5 μM As_2O_3 exposure, leaving nominal expression for the 2.5 μM As_2O_3 exposure. Analysis of PCAF expression at the 3-hour time point was able to identify a significant increase in PCAF expression, whilst at the longer 72-hour exposure PCAF expression was suppressed at both tolerated and toxic dosages (Figure. 2, F).

Effects of E2F1 binding and H3K9 acetylation at selected gene promoters in response to As_2O_3

To assess the relationship between histone acetylation and the transcriptional regulation of apoptotic genes and proto-oncogenes we focused on the transcription factor E2F1, which has been shown to influence decisions between cellular proliferation and cell death (Chen et al.

1985; Hallstrom et al. 2008). E2F1 and H3K9 acetylation interactions at a number of gene promoters including the tumour suppressor (*p53*), apoptotic genes (*Bax & Puma*) and proto-oncogenes (*Myc* & *Fos*) were assessed by chromatin immunoprecipitation and quantitative real-time polymerase chain reaction (qRT-PCR).

HEK293T cells were exposed to As_2O_3 for 3 and 72 hours. After 3 hours of exposure there was a significant enrichment of the *FOS* promoter fragment with 0.5 μM As_2O_3 treatment after precipitation with an anti-acetylated H3K9 antibody (Figure. 3, A). This suggests an increase in H3K9 acetylation at the *FOS* promoter. Using the same duration of exposure and an anti-E2F1 antibody, enrichment at the *FOS* promoter was observed at both 0.5 μM and 2.5 μM As_2O_3 treatments, suggesting increased binding of E2F1 to the *FOS* promoter (Figure. 3, B). After 72-hours exposure, dosage specific responses were identified where significantly elevated binding to the *FOS* promoter occurred specifically at the tolerated 0.5 μM As_2O_3 treatment with both E2F1 and H3K9 acetylated antibody pull-downs (Figure. 3, C, D). The same dosage-specific response was validated in the UROtsa cell line, where tolerated 72-hour exposure to tolerated 1 μM As_2O_3 led to a significantly elevated binding of acetylated H3K9 and E2F1 at the *FOS* promoter fragment (Figure. 3, E, F).

The relative enrichment of PCAF and HDAC2 at the *FOS* promoter was also investigated after a 72-hour exposure to determine if these enzymes are involved in the maintenance of H3K9 acetylation (Figure. 3, G, H). At the tolerated 0.5 μM As_2O_3 there was increased binding of PCAF at the *FOS* promoter and also at the toxic 2.5 μM As_2O_3 treatments. There was no significant difference in the HDAC2 binding at either exposure.

Effects of As_2O_3 on *JUN*, *MDM2*, and *FOS* expression

The effect of arsenic on the expression of the proto-oncogenes *Jun*, *Fos* and *Mdm2* was measured by qRT-PCR. The over-expression of these genes are synonymous with cancer stem cell expansion, p53 regulation and proliferation (Ito et al. 2002; Jiao et al. 2010).

After 3-hours of exposure, the expressional changes observed are subtle with a significant increase only in *Jun* expression with the 2.5 μM As_2O_3 treatment (Figure. 3, I). After 72-hours of exposure the differences are more pronounced between the tolerated and toxic exposures. This is highlighted by the expression of *FOS*, which is highly elevated at the 0.5 μM As_2O_3 exposure. This increase was dosage-specific, as the toxic 2.5 μM As_2O_3 exposure resulted in no significant elevation. A similar expression pattern was observed for *Jun*. A significantly elevated expression of the *FOS* and *JUN* mRNA was also reported in the UROtsa cell line after tolerated 1 μM As_2O_3 after 72 hours (Figure. 3, J). The expression of *MDM2 mRNA* was significantly increased at the tolerated 0.5 μM As_2O_3 exposure in the HEK293T cell line.

Differential effects of tolerated and toxic arsenic trioxide exposures on global chromatin conformation

A micrococcal nuclease sensitivity assay was used to assess global chromatin conformation. Rapid relaxation occurred after 3-hours with 0.5 μM and 2.5 μM As_2O_3 exposures as the digestion pattern was positively skewed towards the 250 to 500 base pair size range, relative to the 2,000 base pair size (Figure. 4, A). The 2.5 μM As_2O_3 treatment led to greater chromatin relaxation than the 0.5 μM As_2O_3 treatment after 3-hours. This relaxation was reversed after 72-hours, where the toxic 2.5 μM As_2O_3 treatment led to chromatin condensation (Figure. 4, B). At 72-hours the tolerated 0.5 μM As_2O_3 exposure has the same digestion pattern as the control, with

the majority of the DNA in the 2,000 base pair size range, with a small elevation in the 250 base pair range compared to the control.

Discussion

In this study we describe an *in vitro* framework to identify a tolerated dosage of As_2O_3 that induces cellular transformation as an important prerequisite to epigenetic characterisation. To our knowledge this initial dosage determination with knowledge of cellular outcome followed by the measurement of epigenetic parameters is undocumented. Multiple cellular transformation indicators ensured selection of the correct dosage and duration of exposure. In the absence of arsenic, cells showed no signs of deterioration or apoptosis indicating that the culture conditions used were well tolerated. Cell line specific tolerated and toxic dosages were determined. Both 0.5 μM and 2.5 μM As_2O_3 were tolerated at 3 hours in HEK293T cells, but at 72 hours they became tolerated and toxic respectively. In UROtsa cells 1 μM and 5 μM As_2O_3 were tolerated and toxic respectively at 72 hours. Both toxic exposures stimulated apoptosis after a 72-hour exposure. In contrast, tolerated exposures were shown to potentiate transformative properties including positive proliferation and a redistributed cell cycle to pass through the G1/S and G2/M checkpoints in both cell lines. Increased cellular survival and an elevated number of colonies grown under anchorage-independent conditions were observed in HEK293T cells after a tolerated exposure.

These findings further our understanding of the paradoxical effects of arsenic trioxide as an anticancer agent and carcinogen. Whilst it may be effective for some malignancies, As_2O_3 treatment may not be appropriate for kidney and urothelial cancers as we have shown tolerated exposures may lead to cellular transformation rather than cell death. The dichotomy of arsenicals

as a potent cancer treatment and carcinogenic compound is still under intense investigation. Additional insights into these effects have attempted to compare and contrast the toxicity of multiple arsenicals. Human lung adenocarcinoma A549 cells treated with 15 μM sodium arsenite ($NaAsO_2$) led to an increase of cells passing the G1/S checkpoint, in contrast a 15 μM As_2O_3 which led to a significant decrease, suggesting that sodium arsenite is potentially more carcinogenic (Jiang et al. 2013). Doses lower than 5 μM were not a focus of this study and the exposure duration was 24 hours, leading to toxic cellular outcomes. Another study compared As_2O_3, $NaAsO_2$ and monomethylarsonous acid [MMA(III)] toxicity in the context of zinc finger peptides and found that the latter changed the conformation and displaced zinc in C2H2, C3H1 and C4 zinc finger proteins isolated from human keratinocyte HaCaT cells (Zhou et al. 2014). These studies demonstrate toxicity and carcinogenicity variations dependent on the species of arsenic, which is in addition to this present study that suggests the dosage and duration of exposure is significant also.

Using tolerated and toxic dosages we report temporally sensitive changes in global H3K9, H4K12 and H4K16 acetylation as a result of tolerated arsenic trioxide exposure in both cell lines. Prior research has identified a mixture of promoter specific and global histone acetylation changes. Altered histone H3 acetylation patterns in the *DBC1*, *FAM83A*, *ZSCAN12* and *C1QTNF6* gene promoters has been reported as a result of exposure to an intermediate of arsenic catabolism, monomethylarsonous acid MMA(III) (Jensen et al. 2008). Our observed reduction of H4K16 acetylation, although not significant is in concert with previous research where a decreasing H4K16 acetylation profile after chronic exposure to 3 μM As_2O_3 and 1 μM MMA(III) is believed to protect cells from arsenic toxicity (Jo et al. 2009). Urinary arsenic concentration and H3K9 acetylation in peripheral blood mononuclear cells are inversely

correlated, which is concomitant with our observed hypo-acetylation of H3K9 at both tolerated and toxic exposures with both cell lines at 72 hours (Chervona et al. 2012). Our data suggests that hypo-acetylation of H3K9 and H4K16 may be involved in the intermediary steps towards cellular transformation. These endpoints alone however did not give clear mechanistic separation between tolerated and toxic outcomes as both exposures induced hypo-acetylation.

We interrogated the association between hypo-acetylation and cellular transformation by identifying the enzymes HDAC2 and PCAF as regulators of H3K9 acetylation in HEK293T cells. Subsequent investigation into HDAC2 and PCAF mRNA levels by qRT-PCR, demonstrated that the initial increase in global H3K9 acetylation is potentially caused by an adjustment in the HDAC2 to PCAF expression ratio. The direction of this imbalance is inverted at the 72-hour time point, where at the tolerated exposure of 0.5 μM As_2O_3, HDAC2 expression is significantly elevated combined with a significant reduction in PCAF expression leading to global hypo-acetylation of the H3K9 residue at the 72-hour time point in HEK293T cells.

Although aberrant PCAF and HDAC2 expression in the context of arsenic-induced carcinogenicity has not yet been documented, both PCAF and HDAC2 have been implicated in cancer. The role of PCAF is not definitive in carcinogenesis, but there is growing consensus that PCAF has tumour suppressive properties (Zheng et al. 2013). HDAC2 is also believed to interact with cell cycle components, where siRNA-mediated silencing of HDAC2, inhibits progression through the G1/S checkpoint in hepatocarcinoma cells (Noh et al. 2011). This is particularly significant as tolerated As_2O_3 exposure led to a redistributed cell cycle to favour cellular proliferation by passing both G1/S and G2/M checkpoints in both cell lines.

To assess the significance of global H3K9 hypo-acetylation in the transcriptional control of proto-oncogenes and apoptotic genes, chromatin immunoprecipitation was used to focus on the transcription factor E2F1, due to its dual role in proliferation and apoptosis (Korah et al. 2012). We investigated the binding of E2F1 at a number of promoters and identified the co-occurrence of promoter-specific H3K9 acetylation and E2F1 at the *FOS* promoter, a well-established proto-oncogene in HEK293T and UROtsa cells. At the 72-hour time point this interaction was significantly strengthened at the tolerated concentration. E2F1 has been previously shown to interact in the promoter region of *FOS* and the retinoblastoma control element (RCE) and regulate the transcription of the pRb protein, an important regulatory protein in balancing cellular proliferation and apoptosis (Mimaki et al. 2005). At 3 hours H3K9 is hyper-acetylated at the *FOS* promoter similar to the global acetylation profile. This localised acetylation is able to stimulate significant E2F1 binding at both tolerated and toxic exposures. This adjusts after 72 hours of exposure, as H3K9 acetylation is maintained at the *FOS* promoter specifically at the tolerated treatment in both cell lines, and although global H3K9 acetylation is reduced at this exposure, E2F1 transcription factor binding is still secure at the *FOS* promoter leading to transcription. It has been previously documented that E2F1 is able to recruit other histone acetyltransferases such as GCN5 to acetylate localised H3K9 residues (Guo et al. 2011). We predict that a potentially similar mechanism is involved as we identified elevated binding of PCAF at the *FOS* promoter in concert with E2F1 after a tolerated treatment of 72 hours. This allowed for the maintained H3K9 acetylation at the promoter. Although a similar increase in PCAF binding is observed at the toxic exposure, this does not occur with E2F1 binding at the promoter, leaving *FOS* expression and H3K9 acetylation nominal. Furthermore, combined

transfection with PCAF and treatment at the toxic dosage, leads to inhibited acetylation activity on the H3K9 substrate compared to transfected untreated controls.

Our data demonstrates how arsenic-induced changes in global histone acetylation are not always reflected at the promoter specific level. Rather early perturbations in global histone acetylation, lead to transcription factor binding and promoter specific effects. In our proposed mechanism arsenic exposure leads to an adjustment in HDAC2 and PCAF expression and hyper-acetylation of the H3K9 residue within 3 hours (Figure. 4, C). This may allow for the early recruitment of E2F1, which after 72-hours leads to PCAF mediated H3K9 hyper-acetylation at the promoter and sustained transcription. This promoter specific effect occurs against a background of global H3K9 hypo-acetylation. This understanding of arsenic-induced global acetylation information followed by focused profiling at a specific gene promoter loci is a significant step in understanding arsenic-induced carcinogenesis from perturbations in histone post-translational status.

Transcriptional regulation and higher order chromatin conformation are intrinsically tethered by histone acetylation events which adjust the electrostatic properties of the histones (Shogren-Knaak 2006). We report chromatin relaxation in a dose-dependent manner in addition to increases in H3K9 and H4K12 acetylation at the 3-hour time point in HEK293T cells. Extension of the exposure to 72 hours led to chromatin condensation in the toxic exposure but normalisation of the chromatin architecture at the tolerated exposure in HEK293T cells. This demonstrates the reversibility of initial relaxation and this co-occurs with the global hypo-acetylation of H3K9 and normalisation of H412 acetylation in HEK293T cells. Similar condensation is observed as a result of arsenic trioxide initiated apoptosis in the treatment of hepatocarcinoma (Alarifi et al. 2013). This may explain why initial E2F1 binding at the toxic

exposure does not maintain after a 72-hour exposure, as the chromatin is severely condensed and E2F1 binding becomes unfavourable at the *FOS* promoter. We also measured the mRNA levels of other proto-oncogenes *JUN* and *MDM2*, both of which after 72 hours exhibit significantly elevated expression at the tolerated As_2O_3 exposure, further contributing to cellular transformation.

Conclusions

This study presents additional mechanistic detail to arsenic-induced cellular transformation by starting with the analysis of histone post-translation modifications. We believe that global histone acetylation changes and promoter specific impacts are not entirely congruent and rather promoter specific histone acetylation changes are more accurate in separating the opposing physiological outcomes of cellular transformation and toxicity. In summary, this research outlined a framework for interrogating arsenic-induced carcinogenesis, by utilising a clear dosage selection methodology. Tolerated As_2O_3 exposure leads to early H3K9 acetylation increase in HEK293T and UROtsa cells mediated by an imbalance in the intracellular HDAC2 to PCAF expression ratio as observed in HEK293T cells. This event allows for the subsequent binding of E2F1 at the *FOS* promoter, which maintains promoter-localised H3K9 acetylation, against the global H3K9 hypo-acetylation trend observed at the tolerated exposure in both cell lines. We also report short-term arsenic trioxide induced chromatin relaxation in HEK293T cells and then a return to nominal levels for the tolerated concentration in contrast to the toxic exposure, which leads to clear chromatin condensation and apoptosis. The identification of more promoter targets regulated by histone acetylation as a result of tolerated As_2O_3 exposure may help to further our understanding of arsenic-induced cellular transformation.

References

Alarifi S, Ali D, Alkahtani S, Siddiqui MA, Ali BA. 2013. Arsenic trioxide-mediated oxidative stress and genotoxicity in human hepatocellular carcinoma cells. Onco Targets Ther 6:75–84; doi:10.2147/OTT.S38227.

Bookout AL, Cummins CL, Mangelsdorf DJ, Pesola JM, Kramer MF. 2006. High-throughput real-time quantitative reverse transcription PCR. Curr Protoc Mol Biol Chapter 15:Unit–Uni8; doi:10.1002/0471142727.mb1508s73.

Cold Spring Harbor Laboratory Press. 2005. Micrococcal nuclease–Southern blot assay. Nature Methods. 2:719–720; doi:10.1038/nmeth0905-719.

Chanda S. 2006. DNA Hypermethylation of Promoter of Gene p53 and p16 in Arsenic-Exposed People with and without Malignancy. Toxicological Sciences 89:431–437; doi:10.1093/toxsci/kfj030.

Chen CJ, Chuang YC, Lin TM, Wu HY. 1985. Malignant neoplasms among residents of a blackfoot disease-endemic area in Taiwan: high-arsenic artesian well water and cancers. Cancer Research 45:5895–5899.

Chervona Y, Hall MN, Arita A, Wu F, Sun H, Tseng H-C, et al. 2012. Association Between Arsenic Exposure and Global Post-translational Histone Modifications Among Adults in Bangladesh. Cancer Epidemiol. Biomarkers Prev.; doi:10.1158/1055-9965.EPI-12-0833.

Duriez PJ, Shah GM. 1997. Cleavage of poly(ADP-ribose) polymerase: a sensitive parameter to study cell death. Biochem. Cell Biol. 75:337–349; doi:10.1139/bcb-75-4-337.

Füllgrabe J, Hajji N, Joseph B. 2010. Cracking the death code: apoptosis-related histone modifications. Cell Death Differ. 17:1238–1243; doi:10.1038/cdd.2010.58.

Grund SC, Hanusch K, Wolf HU. 2008. Arsenic and Arsenic Compounds - Ullmann's Encyclopedia of Industrial Chemistry. onlinelibrary.wiley.com; doi:10.1002/14356007.a03_113.pub2. Available: http://onlinelibrary.wiley.com/doi/10.1002/14356007.a03_113.pub2/pdf [accessed 26 April 2011].

Guo R, Chen J, Mitchell DL, Johnson DG. 2011. GCN5 and E2F1 stimulate nucleotide excision repair by promoting H3K9 acetylation at sites of damage. Nucleic Acids Research 39:1390–1397; doi:10.1093/nar/gkq983.

Hajji N, Wallenborg K, Vlachos P, llgrabe JFU, Hermanson O, Joseph B. 2010. Opposing effects of hMOF and SIRT1 on H4K16 acetylation and the sensitivity to the topoisomerase II inhibitor etoposide. Oncogene 29:2192–2204; doi:10.1038/onc.2009.505.

Hallstrom TC, Mori S, Nevins JR. 2008. An E2F1-Dependent Gene Expression Program that Determines the Balance between Proliferation and Cell Death. Cancer Cell 13:11–22; doi:10.1016/j.ccr.2007.11.031.

Iacobuzio-Donahue CA. 2009. Epigenetic Changes in Cancer. Annu. Rev. Pathol. Mech. Dis. 4:229–249; doi:10.1146/annurev.pathol.3.121806.151442.

Ito A, Kawaguchi Y, Lai C-H, Kovacs JJ, Higashimoto Y, Appella E, et al. 2002. MDM2-HDAC1-mediated deacetylation of p53 is required for its degradation. EMBO J. 21:6236–6245.

Jensen TJ, Novak P, Eblin KE, Gandolfi AJ, Futscher BW. 2008. Epigenetic remodeling during arsenical-induced malignant transformation. Carcinogenesis 29:1500–1508; doi:10.1093/carcin/bgn102.

Jiang X, Chen C, Zhao W, Zhang Z. 2013. Sodium arsenite and arsenic trioxide differently affect the oxidative stress, genotoxicity and apoptosis in A549 cells: an implication for the paradoxical mechanism. Environ. Toxicol. Pharmacol. 36:891–902; doi:10.1016/j.etap.2013.08.002.

Jiao X, Katiyar S, Willmarth NE, Liu M, Ma X, Flomenberg N, et al. 2010. c-Jun Induces Mammary Epithelial Cellular Invasion and Breast Cancer Stem Cell Expansion. Journal of Biological Chemistry 285:8218–8226; doi:10.1074/jbc.M110.100792.

Jo WJ, Ren X, Chu F, Aleshin M, Wintz H, Burlingame A, et al. 2009. Acetylated H4K16 by MYST1 protects UROtsa cells from arsenic toxicity and is decreased following chronic arsenic exposure. Toxicol. Appl. Pharmacol. 241:294–302; doi:10.1016/j.taap.2009.08.027.

Kapaj S, Peterson H, Liber K, Bhattacharya P. 2006. Human Health Effects From Chronic Arsenic Poisoning–a Review. Journal of Environmental Science and Health, Part A: Toxic/Hazardous Substances & Environmental Engineering 41:2399–2428; doi:10.1080/10934520600873571.

Kim H-G, Kim DJ, Li S, Lee KY, Li X, Bode AM, et al. 2012. Polycomb (PcG) proteins, BMI1 and SUZ12, regulate arsenic-induced cell transformation. Journal of Biological Chemistry 287:31920–31928; doi:10.1074/jbc.M112.360362.

Korah J, Falah N, Lacerte A, Lebrun JJ. 2012. A transcriptionally active pRb-E2F1-P/CAF signaling pathway is central to TGFβ-mediated apoptosis. Cell Death Dis 3:e407; doi:10.1038/cddis.2012.146.

Kurttio P, Pukkala E, Kahelin H, Auvinen A, Pekkanen J. 1999. Arsenic concentrations in well water and risk of bladder and kidney cancer in Finland. Environ Health Perspect 107:705–710.

Li J, Chen P, Sinogeeva N, Gorospe M, Wersto RP, Chrest FJ, et al. 2002. Arsenic trioxide promotes histone H3 phosphoacetylation at the chromatin of CASPASE-10 in acute promyelocytic leukemia cells. J. Biol. Chem. 277:49504–49510; doi:10.1074/jbc.M207836200.

Liu Y, Hock JM, Sullivan C, Fang G, Cox AJ, Davis KT, et al. 2010. Activation of the p38 MAPK/Akt/ERK1/2 signal pathways is required for the protein stabilization of CDC6 and cyclin D1 in low-dose arsenite-induced cell proliferation. J. Cell. Biochem. 111:1546–1555; doi:10.1002/jcb.22886.

Mimaki S, Mori-Furukawa Y, Katsuno H, Kishimoto T. 2005. A transcriptional regulatory element screening system reveals a novel E2F1/pRb transcription regulation pathway. Analytical Biochemistry 346:268–280; doi:10.1016/j.ab.2005.08.021.

Nelson JD, Denisenko O, Bomsztyk K. 2006. Protocol for the fast chromatin immunoprecipitation (ChIP) method. Nat Protoc 1:179–185; doi:10.1038/nprot.2006.27.

Niedzwiecki MM, Hall MN, Liu X, Oka J, Harper KN, Slavkovich V, et al. 2013. A Dose-Response Study of Arsenic Exposure and Global Methylation of Peripheral Blood Mononuclear Cell DNA in Bangladeshi Adults. Environ Health Perspect 121:1306–1312; doi:10.1289/ehp.1206421.

Noh JH, Jung KH, Kim JK, Eun JW, Bae HJ, Xie HJ, et al. 2011. Aberrant Regulation of HDAC2 Mediates Proliferation of Hepatocellular Carcinoma Cells by Deregulating Expression of G1/S Cell Cycle Proteins. PLoS ONE 6:e28103; doi:10.1371/journal.pone.0028103.

Peserico A, Simone C. 2011. Physical and Functional HAT/HDAC Interplay Regulates Protein Acetylation Balance. Journal of Biomedicine and Biotechnology 2011:1–10; doi:10.1155/2011/371832.

Raptis L, Vultur A. 2001. Neoplastic transformation assays. Methods Mol. Biol. 165:151–164.

Reichard JF, Puga A. 2010. Effects of arsenic exposure on DNA methylation and epigenetic gene regulation. Epigenomics 2:87–104; doi:10.2217/epi.09.45.

Ren X, McHale CM, Skibola CF, Smith AH, Smith MT, Zhang L. 2011. An emerging role for epigenetic dysregulation in arsenic toxicity and carcinogenesis. Environ Health Perspect 119:11–19; doi:10.1289/ehp.1002114.

Rossi MR, Masters JR, Park S, Todd JH, Garrett SH, Sens MA, et al. 2001. The immortalized UROtsa cell line as a potential cell culture model of human urothelium. Environ Health Perspect 109:801–808.

Shi H, Shi X, Liu KJ. 2004. Oxidative mechanism of arsenic toxicity and carcinogenesis. Mol. Cell. Biochem. 255:67–78.

Shogren-Knaak M. 2006. Histone H4-K16 Acetylation Controls Chromatin Structure and Protein Interactions. Science 311:844–847; doi:10.1126/science.1124000.

Soignet SL, Maslak P, Wang ZG, Jhanwar S, Calleja E, Dardashti LJ, et al. 1998. Complete remission after treatment of acute promyelocytic leukemia with arsenic trioxide. N. Engl. J. Med. 339:1341–1348; doi:10.1056/NEJM199811053391901.

Stueckle TA, Lu Y, Davis ME, Wang L, Jiang B-H, Holaskova I, et al. 2012. Chronic occupational exposure to arsenic induces carcinogenic gene signaling networks and neoplastic transformation in human lung epithelial cells. Toxicol. Appl. Pharmacol. 261:204–216; doi:10.1016/j.taap.2012.04.003.

Zheng X, Gai X, Ding F, Lu Z, Tu K, Yao Y, et al. 2013. Histone acetyltransferase PCAF Up-regulated cell apoptosis in hepatocellular carcinoma via acetylating histone H4 and inactivating AKT signaling. Mol Cancer 12:96; doi:10.1186/1476-4598-12-96.

Zhou X, Sun H, Ellen TP, Chen H, Costa M. 2008. Arsenite alters global histone H3 methylation. Carcinogenesis 29:1831–1836; doi:10.1093/carcin/bgn063.

Zhou X, Sun X, Mobarak C, Gandolfi AJ, Burchiel SW, Hudson LG, et al. 2014. Differential binding of monomethylarsonous acid compared to arsenite and arsenic trioxide with zinc finger peptides and proteins. Chem. Res. Toxicol. 27:690–698; doi:10.1021/tx500022j.

Figure Legends

Figure 1. Biochemical and flow-cytometric analysis based identification of a tolerated and toxic exposure of As_2O_3 and cellular transformation assays in HEK293T and UROtsa cell lines. (A) Immunoblotting for PARP cleavage after 24 hours exposure. (B) Immunoblotting for MDM2, p53 activation, caspase-3 cleavage and apoptotic-relay signals after 1-week exposure. (C) Immunoblotting for PARP cleavage after 1-week exposure. (D) Immunoblotting for PARP cleavage after 72-hour exposure. (E) Flow cytometry to quantify mitochondrial ROS after 72 hours exposure. (F) Flow cytometry to measure mitochondrial membrane depolarisation, $\Delta\Psi_m$ after 72 hours exposure. (G) Flow cytometry to quantify propidium iodide bound DNA after 72 hours exposure. (H, I) WST-1 Proliferation Assay conducted to determine the proliferative index of the treated cells. HEK293T cells were treated with 0.5 μM and 2.5 μM As_2O_3, whilst UROtsa cells were treated with 1 μM and 5 μM As_2O_3 for 3 hours, 72 hours and 1-week. (J, K) Cell-cycle analysis of HEK293T cells after exposure to 0.5 μM and 2.5 μM As_2O_3 and UROtsa cells after exposure to 1 μM and 5 μM As_2O_3 for 72-hours using propidium iodide staining followed by flow cytometric analysis. (L) 15-day exposure clonogenic assay, scanned image shows the number and approximate size of colonies after exposure with 0.5μM and 2.5 μM As_2O_3. (M) 15-day exposure clonogenic assay with survival fraction quantified after triplicate counting of 0.5 μM and 2.5 μM As_2O_3 treated cells. (N, O) Phase contrast images (10x) and counts of colonies grown in soft-agar after a 12-week exposure period to 0.5 μM. Statistical significance is depicted by * for $p<0.05$ calculated by a two-tailed Student's T test compared to the untreated control group with N=3. All bars plotted are mean ± SD.

Figure 2. Histone acetylation analysis of HEK293T and UROtsa cells, identification of H3K9 acetylation control and mRNA expression analysis of HDAC2 and PCAF at 3 hours and 72 hours. (A, B) Histone acetylation of H3K9, H4K12 and H4K16 analysed by immunoblotting. All changes are plotted as mean ± SD after densitometry analysis as described in "Materials and Methods." (C) H3K9 acetylation status analysed by immunoblotting after transfection with HDAC1, 2, 3 and 4 followed by histone extraction to examine the relative enzymatic effect of these HDACs on this residue. Blots were quantified by densitometry analysis and plotted as mean ± SD from three independent experiments. (D) H3K9 acetylation status after transfection with a no-insert control and PCAF followed by a 3 hour exposure to 0.5 μM and 2.5 μM As_2O_3.

(E, F) Relative mRNA expression ratios, expressed as fold change for HDAC2 and PCAF for two time points, 3 hours and 72 hours. Statistical significance is depicted by * for $p<0.05$ calculated by a two-tailed Student's T test compared to the untreated control group of N=3 (A, B, E) and N=4 (F, 3 hours). All bars plotted are mean ± SD.

Figure 3. Tolerated exposure induces the expression of JUN, FOS and MDM2 and leads to the recruitment of E2F1 at the FOS promoter. (A, B, C, D) Chromatin immunoprecpitated with anti-acetylated H3K9 and anti E2F1 antibodies after exposure to 0.5μM and 2.5μM As_2O_3 at two time-points, 3 hours and 72 hours. (E, F) Chromatin immunoprecipitated with anti-acetylated H3K9 and anti E2F1 antibodies after exposure to 1 μM and 5 μM As_2O_3 at 72 hours. (G, H) Chromatin immunoprecipitated with anti HDAC2 and PCAF antibodies at 72 hours. Precipitated chromatin was then subjected to qRT-PCR promoter analysis. (I) Normalised expression ratios are shown for JUN, FOS and MDM2 mRNA. Total RNA was isolated from 0.5μM and 2.5μM As_2O_3 treated HEK293T cells to be used for the qRT-PCR analysis. (J) Normalised expression ratios are shown for JUN and FOS mRNA from UROtsa cells treated with 1 μM As_2O_3 for 72 hours. Statistical significance is depicted by * for $p<0.05$ calculated by a two-tailed Student's T test compared to the untreated control group with N=3. All bars plotted are mean ± SD.

Figure 4. Tolerated and toxic As_2O_3 exposure alters higher order chromatin conformation and a schematic of global and promoter-specific mechanisms in arsenic trioxide-induced cellular transformation. (A, B) MNase sensitivity assay was used to assess the relative levels of chromatin relaxation between two treatments 0.5μM and 2.5μM As_2O_3. Two time-points are shown 3 hours and 72 hours. (C) Schematic mechanism outlining HDAC2 and PCAF mediated global acetylation changes in H3K9 followed by subsequent E2F1 recruitment to the FOS promoter. Tolerated and toxic dosages lead to separated mechanistic outcomes after 72 hours of exposure where a toxic dosage leads to cytotoxicity and chromatin condensation, whilst tolerated exposure leads to continued FOS expression. Tolerated and toxic dosages are abbreviated to the following: "Tol" for 0.5 μM As_2O_3, "Tox.p" (toxic pathway) for 2.5 μM As_2O_3 at 3 hours and "Tox" for 2.5 μM As_2O_3 at ≥ 72 hours in this schematic.

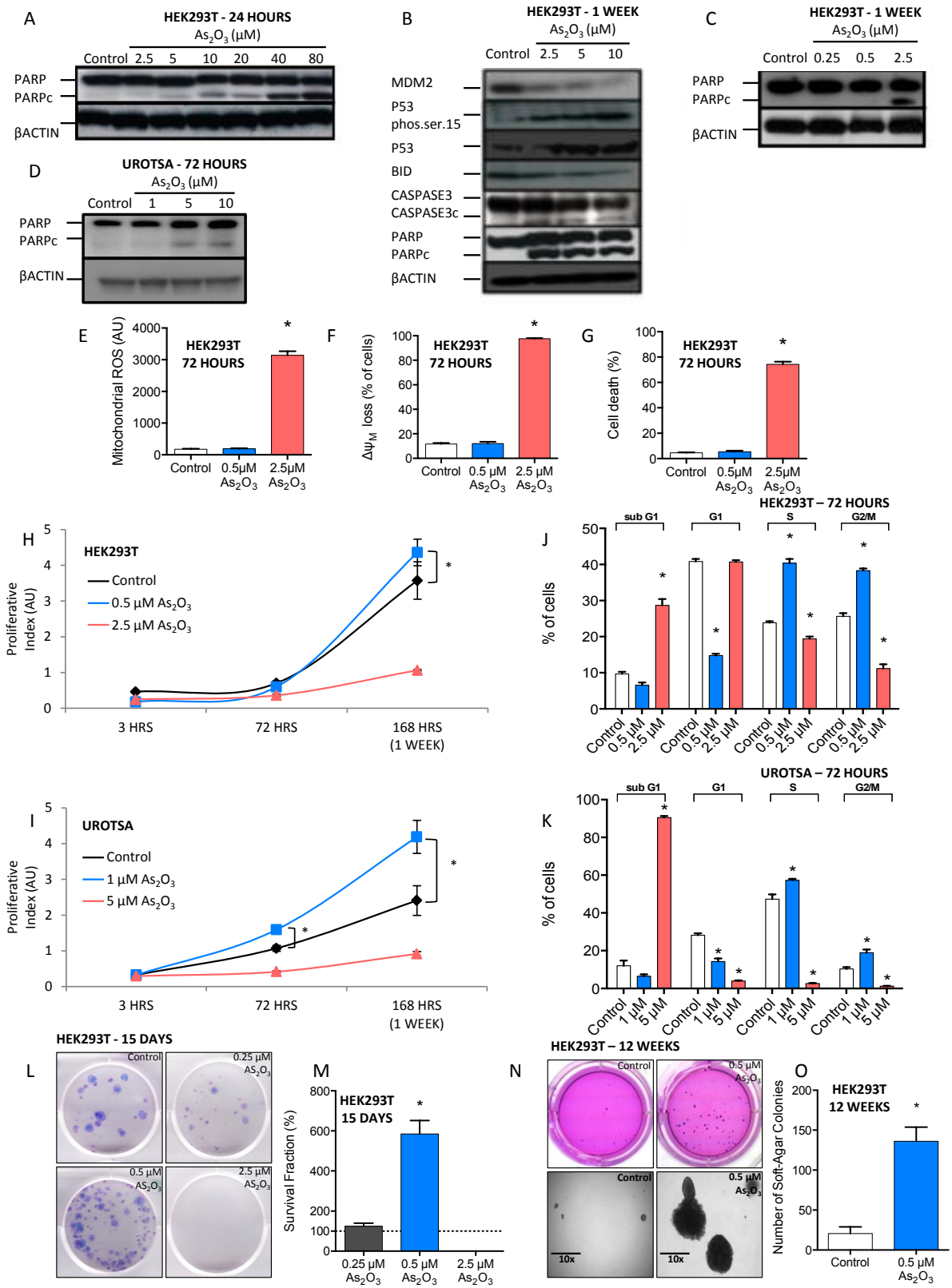
A
HEK293T - 24 HOURS
As2O3 (μM)
Control 2.5 5 10 20 40 80
PARP
PARPc
βACTIN
B
HEK293T - 1 WEEK
As2O3 (μM)
Control 2.5 5 10
MDM2
P53
phos.ser.15
P53
BID
CASPASE3
CASPASE3c
PARP
PARPc
βACTIN
C
HEK293T - 1 WEEK
As2O3 (μM)
Control 0.25 0.5 2.5
PARP
PARPc
βACTIN
D
UROTSA - 72 HOURS
As2O3 (μM)
Control 1 5 10
PARP
PARPc
βACTIN
E
HEK293T
72 HOURS
Mitochondrial ROS (AU)
Control 0.5μM As2O3 2.5μM As2O3
F
HEK293T
72 HOURS
ΔψM loss (% of cells)
Control 0.5 μM As2O3 2.5 μM As2O3
G
HEK293T
72 HOURS
Cell death (%)
Control 0.5μM As2O3 2.5μM As2O3
H
HEK293T
Control
0.5 μM As2O3
2.5 μM As2O3
Proliferative Index (AU)
3 HRS
72 HRS
168 HRS (1 WEEK)
I
UROTSA
Control
1 μM As2O3
5 μM As2O3
Proliferative Index (AU)
3 HRS
72 HRS
168 HRS (1 WEEK)
J
HEK293T – 72 HOURS
sub G1
G1
S
G2/M
% of cells
Control 0.5 μM 2.5 μM
K
UROTSA – 72 HOURS
sub G1
G1
S
G2/M
% of cells
Control 1 μM 5 μM
L
HEK293T - 15 DAYS
Control
0.25 μM As2O3
0.5 μM As2O3
2.5 μM As2O3
M
HEK293T
15 DAYS
Survival Fraction (%)
0.25 μM As2O3 0.5 μM As2O3 2.5 μM As2O3
N
HEK293T – 12 WEEKS
Control
0.5 μM As2O3
Control
0.5 μM As2O3
10x
10x
O
HEK293T
12 WEEKS
Number of Soft-Agar Colonies
Control 0.5 μM As2O3

Figure: 1

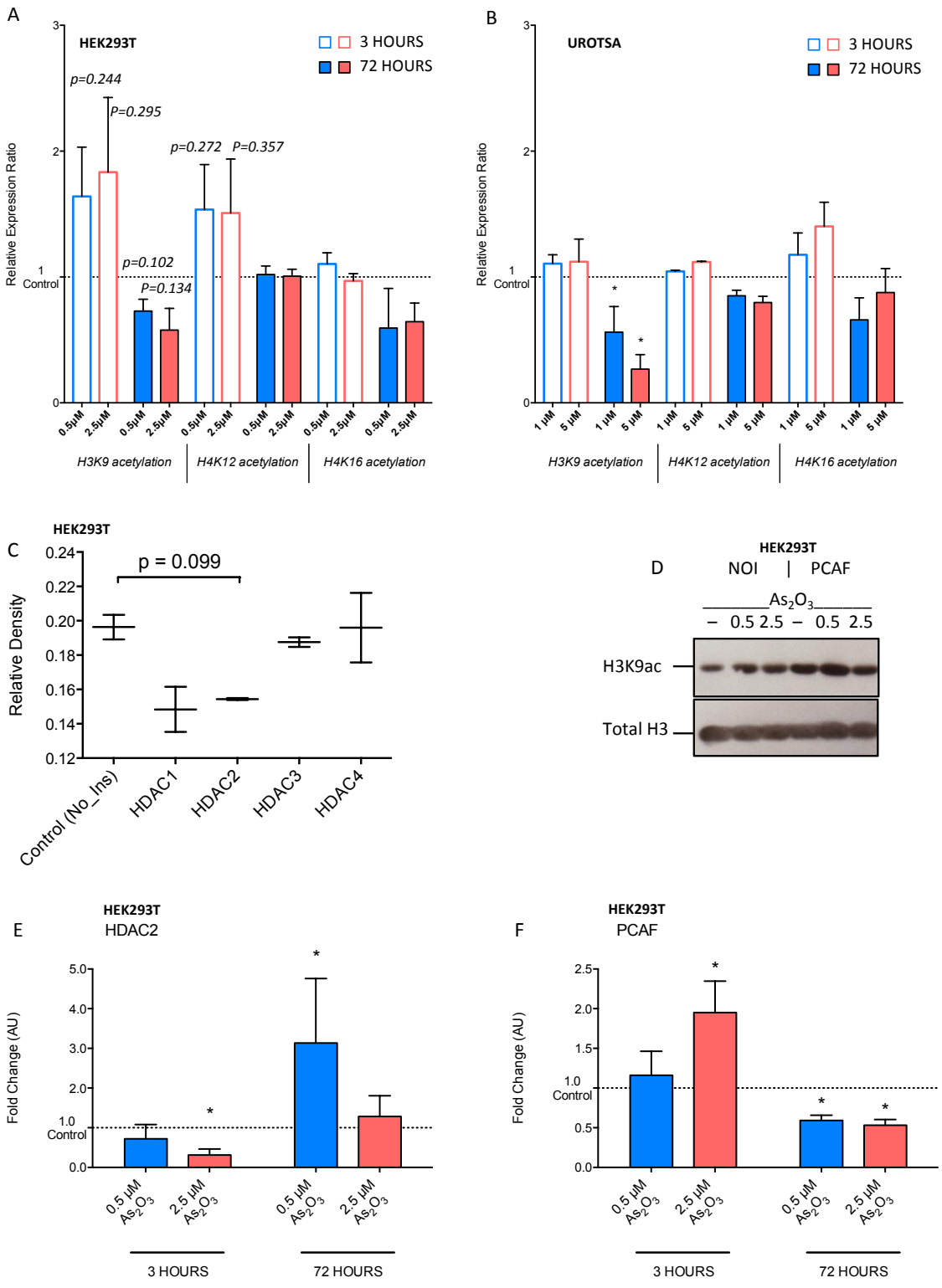
A
HEK293T
3 HOURS
72 HOURS
p=0.244
P=0.295
p=0.272
P=0.357
p=0.102
P=0.134
Relative Expression Ratio
Control
H3K9 acetylation
H4K12 acetylation
H4K16 acetylation
B
UROTSA
C
HEK293T
p = 0.099
Relative Density
Control (No_Ins)
HDAC1
HDAC2
HDAC3
HDAC4
D
HEK293T
NOI | PCAF
As2O3
H3K9ac
Total H3
E
HEK293T
HDAC2
Fold Change (AU)
3 HOURS
72 HOURS
F
HEK293T
PCAF

Figure: 2

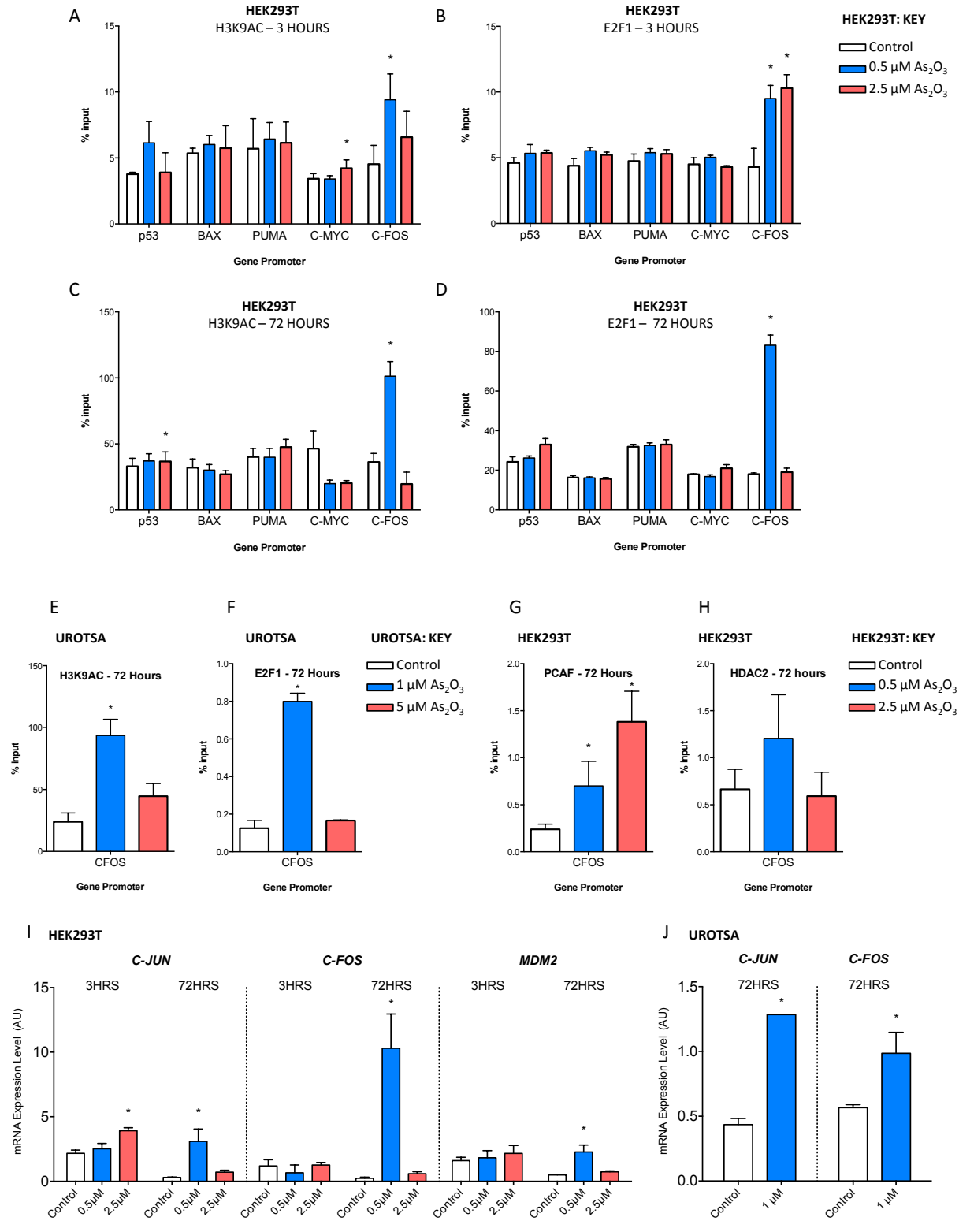
A
HEK293T
H3K9AC – 3 HOURS
% input
p53
BAX
PUMA
C-MYC
C-FOS
Gene Promoter
B
HEK293T
E2F1 – 3 HOURS
HEK293T: KEY
Control
0.5 µM As2O3
2.5 µM As2O3
C
HEK293T
H3K9AC – 72 HOURS
D
HEK293T
E2F1 – 72 HOURS
E
UROTSA
H3K9AC - 72 Hours
CFOS
F
UROTSA
E2F1 - 72 Hours
UROTSA: KEY
1 µM As2O3
5 µM As2O3
G
HEK293T
PCAF - 72 Hours
H
HEK293T
HDAC2 - 72 hours
I
HEK293T
C-JUN
C-FOS
MDM2
3HRS
72HRS
mRNA Expression Level (AU)
Control
0.5µM
2.5µM
J
UROTSA
1 µM

Figure: 3

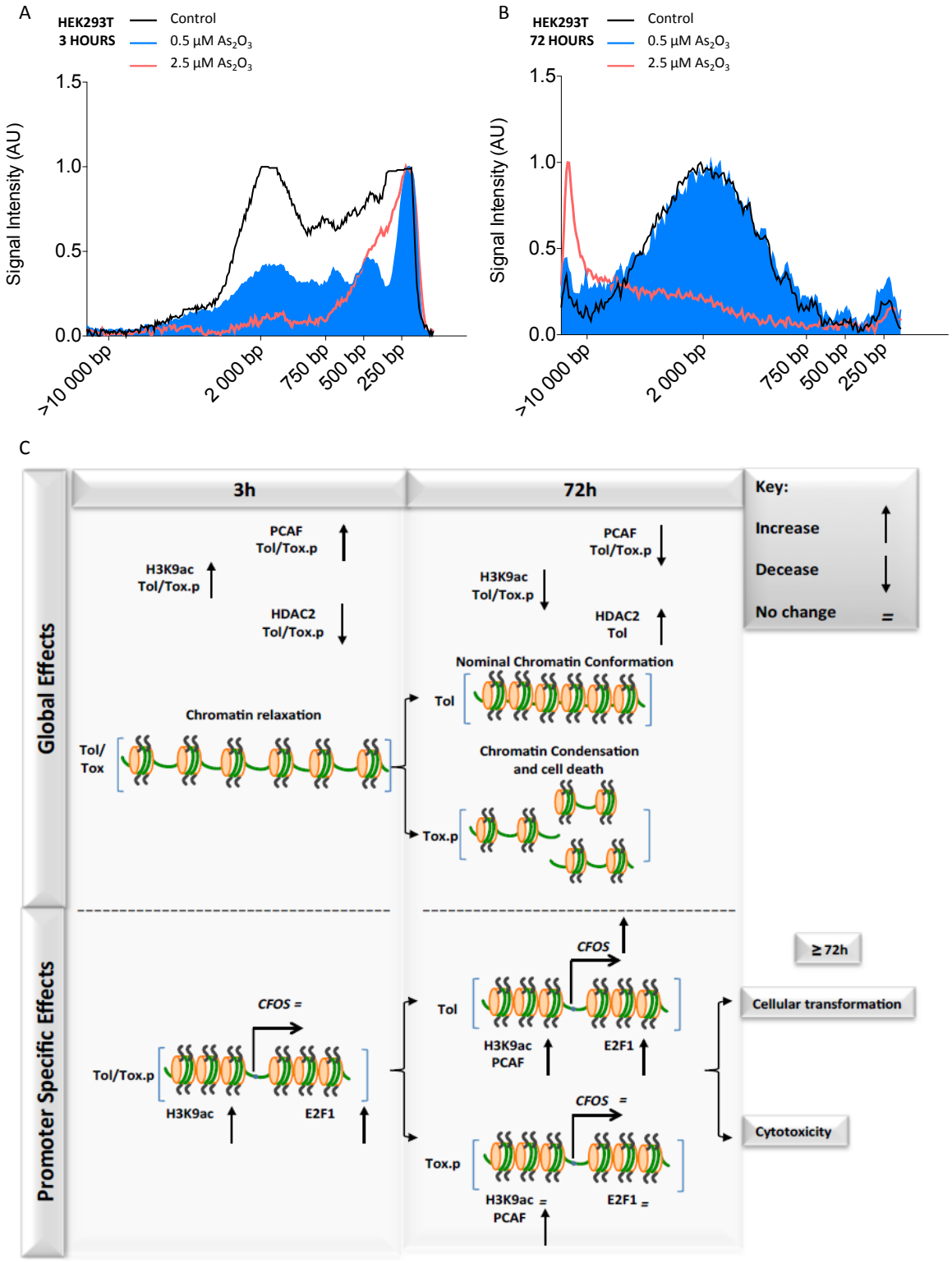
A
HEK293T
3 HOURS
Control
0.5 µM As2O3
2.5 µM As2O3
Signal Intensity (AU)
1.5
1.0
0.5
0.0
>10 000 bp
2 000 bp
750 bp
500 bp
250 bp
B
HEK293T
72 HOURS
Control
0.5 µM As2O3
2.5 µM As2O3
Signal Intensity (AU)
1.5
1.0
0.5
0.0
>10 000 bp
2 000 bp
750 bp
500 bp
250 bp
C
3h
72h
Key:
Increase
Decease
No change
Global Effects
PCAF
Tol/Tox.p
H3K9ac
Tol/Tox.p
HDAC2
Tol/Tox.p
Chromatin relaxation
Tol/
Tox
Nominal Chromatin Conformation
Tol
Chromatin Condensation
and cell death
Tox.p
Promoter Specific Effects
CFOS =
Tol/Tox.p
H3K9ac
E2F1
CFOS
Tol
H3K9ac
PCAF
E2F1
≥ 72h
Cellular transformation
CFOS =
Tox.p
H3K9ac =
PCAF
E2F1 =
Cytotoxicity

Figure: 4